Lattice Gas Automata: Drying Simulation in Heterogeneous Models

D. Jankovic[a*], and D.A. Wolf-Gladrow[b]

[a]Civil Engineering Department, TU Delft,
P.O.Box 5048, 2600 GA Delft, Netherlands

[b]Alfred Wegener Institute for Polar and Marine Research,
Postfach 12 01 61, 27515 Bremerhaven, Germany

Moisture flow in porous media is the driving force behind early age drying shrinkage. Fracture in the interfacial transition zone (ITZ), between cement paste and aggregate-inclusion, is related to restraint caused by, among others, aggregates that obstruct free deformation of the paste. Environmental Scanning Electron Microscope (ESEM) test results are used as a base for the developed method for measuring shrinkage deformations during drying. Modeling of moisture flow in the heterogeneous samples is numerically performed with Lattice Gas Automata (LGA). Fracture coupling of the LGA and Lattice Fracture Model (LFM) requires coupling with ESEM tests regarding shrinkage coefficient.

1. INTRODUCTION

Early age microcracks in concrete, prior to any mechanical load, may be the reason for the serious fractures of reinforced concrete structures in the later phases of their service life. Cracks could be induced by time-dependent variations in the cement paste microstructure [12]. That is probably a result of unavoidable, differential volume changes during drying and development of critical tensile/shear stresses [7], which may exceed the stress threshold, if the strength criterion is assumed. Especially bond cracks emerge due to the weakening of the bond zone (or ITZ), Fig. 1, at a rather young age, depending on curing and drying conditions as well as cement and aggregate properties. In a thickness range of 10-50 μm, the ITZ is a more porous area around aggregate, than the rest of bulk cement paste, and hence with the lowest strength and the highest possibility for cracks to occur [6,8,13]. Although small, compared to the size of concrete composition, ITZ may take 30-50% of the total volume of cement matrix in concrete. Hence, it is important to investigate ITZ, especially when it comes to the flow through ITZ and closely related microcracking [7]. The aim of the numerical part of research is to simulate drying in a model of porous media of 'cement paste' i.e. homogenous sample [9,10] and heterogeneous sample, with embedded solid obstacles. The heterogeneous samples should enable observations of the fictitious moisture behaviour in the close vicinity of the obstacles (defined as ITZ), when their sizes (boundary area), quantity and placement vary.

*2005 O.H.Ammann ASCE/SEI Research Award and the support of Technical University of Delft are gratefully acknowledged

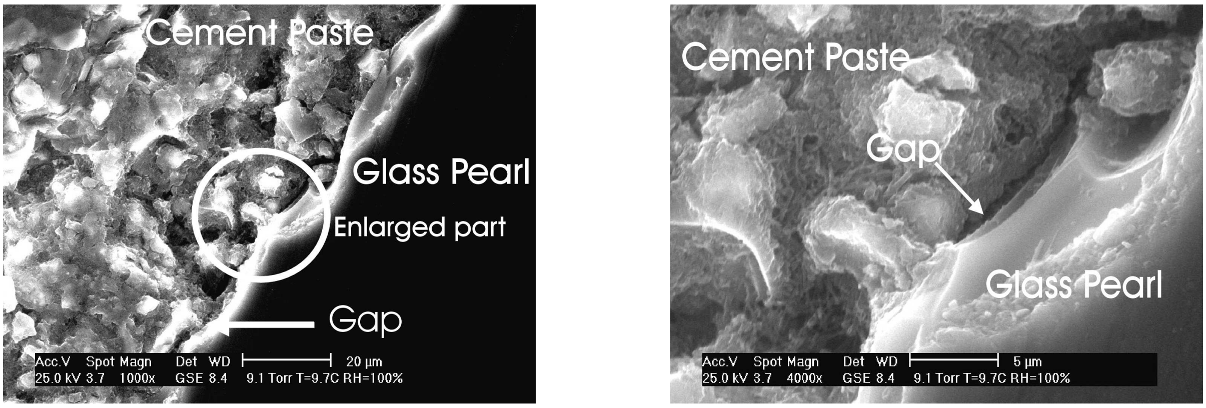

Figure 1. Cement paste with an embedded obstacle (glass pearl) in ESEM digital test (image 1424 x 968 pixels). Microcracking (bond-cracks) in ITZ is visible at the initial stage at 100% RH before drying test takes place: (left) magnified at 20 μm and (right) enlarged to 5 μm [11].

2. MOISTURE FLOW BY MEANS OF LATTICE GAS AUTOMATA

Moisture flow (drying), as the most interesting phenomena that eventually may lead to fracture in cement paste, has been modeled using a 2-D Lattice Gas Automata, LGA. In particular the simple, one-phase FHP model is developed, often described as an exact numerical solution for the Navier-Stokes equation [4].

2.1. Theory of Lattice Gas Automata

Originating from Statistical Mechanics and Cellular Automata [15], LGA bridges the gap between macroscopic and microscopic phenomena. The main Lattice Gas principle is conservation of mass (expressed in a number of fictitious fluid particles) and linear momentum. In order to simulate flow, fluid particles propagate and collide on the regular triangular Bravais lattice following prescribed deterministic and probabilistic rules [5]. The Navier-Stokes equation for incompressible fluid flow is obtained from LGA by Chapman-Enskog expansion [15]. The expansion gives the macroscopic behaviour of fluid by averaging the microscopic (discretized) forms of mass (density) and momentum over the considered area. The macroscopic equations, obtained through the averaging of the mentioned equations, have close similarity to the Navier-Stokes equation for incompressible fluid flow (ρ = const). Detailed derivations can be found in the literature on LGA [4,5,15,3,14].

2.2. FHP, 'heterogeneous' domain, initial and boundary conditions

The domain consists of 1024 x 1024 lattice nodes. In order to observe ITZ as inseparable from aggregate, the domain contains a number of solid, impermeable objects ('obstacles'). The drying is simulated by FHP model [4] with various collision rules. Among others, two sets of collision rules FHP2 (7 cells per node including a particle at rest, 22 collisions) and FHP5 (12 collisions), given in the literature, proved to be a fairly good equivalent to

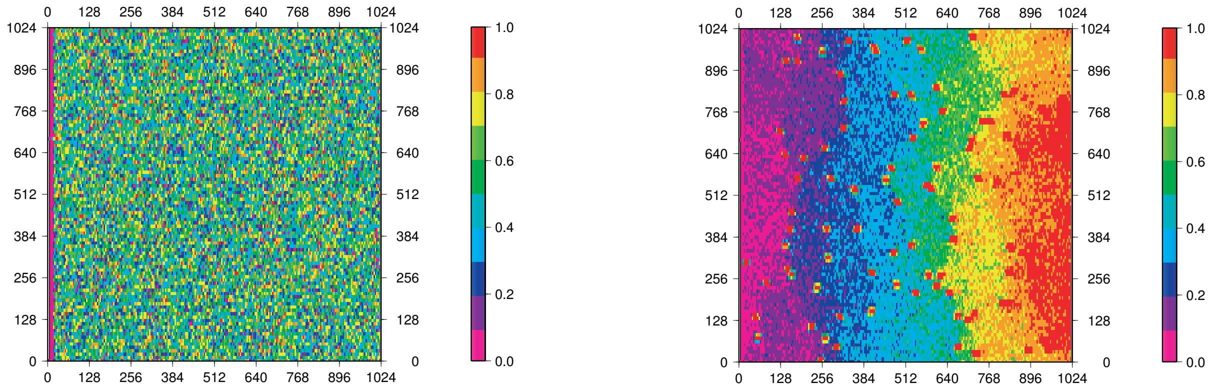

Figure 2. Model 1: simulation of drying in heterogeneous sample with 0.11% of solid obstacles, after 10 (left) and 2000 LGA time-steps (right) with bounce-back reflection as a collision/boundary rule. The moisture content is presented in a scale.

the experimental results [1]. Collision rules in a model influence the viscosity. Compared to FHP5, FHP2 rule induces smaller viscosity, due the higher number of collisions. The wet part of the domain is initialized with a constant mean density (d = 0.85) and thus a fluid at rest. The boundaries of the domain are vertically defined as a default 'periodic' boundary conditions, at the upper and lower boundary. In the horizontal direction, a solid wall is placed, such that the density is kept at a low value, representing the 'surface water pressure', while the model domain is closed at the right. Particles that hit the wall are bounced-back into the domain; bounce-back (no-slip) boundary condition at the solid wall is expressed as r = 0 (r = specular/bounce-back reflection), while r = 1 ratio represents

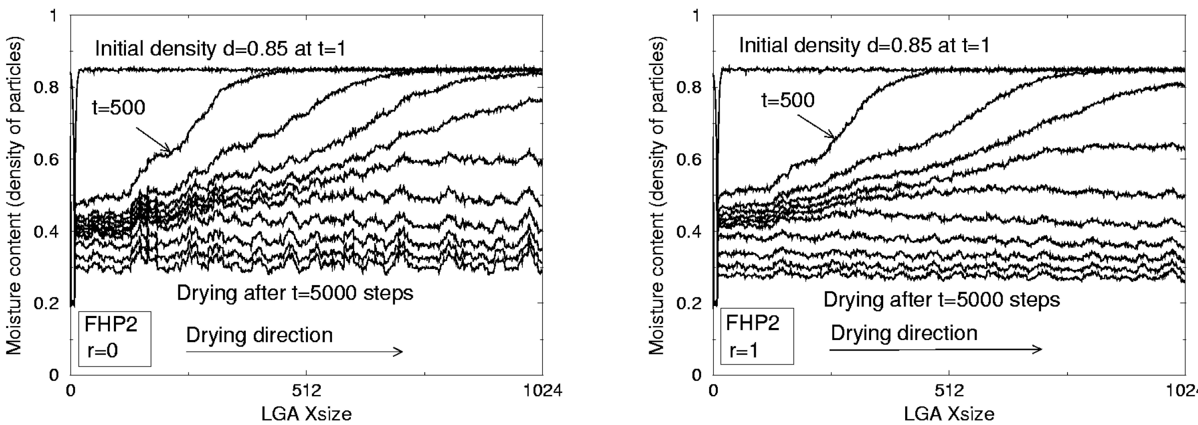

Figure 3. Moisture distribution for model 1, with the built-in solid clusters (20 x 20 lattice sites) with (left) bounce-back rule (r = 0) and (right) specular-reflection rule (r = 1).

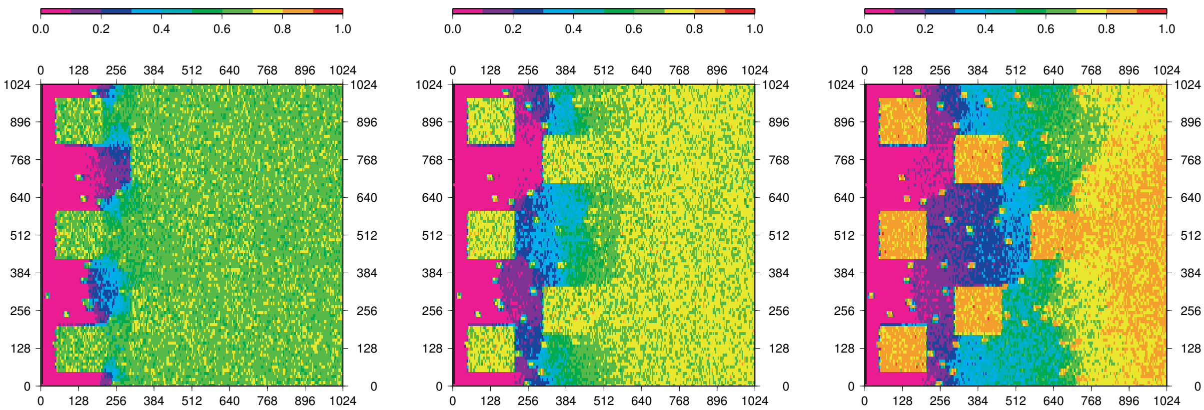

Figure 4. Model 2: Illustration of drying in LGA heterogeneous sample, with embedded six solids and randomly distributed (20 x 20) solid clusters after (left) 500, (middle) 1000 and (right) 2000 LGA time-steps. Applied FHP2 collision rule and bounce-back reflection ($r = 0$) among fluid and solid particles. Moisture content is described in a scale.

the specular-reflection. Particles that cross the open boundary leave the domain and never come back. The loss of particles (moisture) at the open boundary creates a mass density gradient that drives a flow towards the left-hand side. Boundary conditions have to be set also for particles hitting the obstacles that are located inside the domain. Two cases have been studied: a) bounce-back (no-slip) or b) specular-reflection (slip). An increase in the lattice size reduces the statistical noise of the results, but a complete removal of noise in LGA cannot be obtained due to the discretized nature of LGA, which is based on Boolean algebra.

2.3. Discussion of models

Model 1 (small-sized obstacles). The non-homogenous lattice consists of fluid and solid sites (20 x 20 clusters particles, Fig. 2). Simulation of drying runs for 5000 LGA time-steps, starting from the initial density of $d = 0.85$. Bounce-back or specular-reflection, is applied as a boundary condition and the FHP2 collision rule, with 22 collisions (Figs 2,3). Compared to the drying of homogeneous sample of the same lattice size, collision rules and LGA time-step of 500 [12], the results in the heterogeneous lattice are noisier and with less steep moisture gradient. Namely, due to the presence of solids, the moisture gradient decreases but the speed of drying increases (after 5000 LGA steps, the sample is almost dry). The reason could be the boundary condition in the model but also in the real cement paste sample. For example, bounce-back reflection contributes to the noisier but slower drying results (Fig. 3). The opposite is valid for specular-reflection. A certain qualitative agreement could be found between the numerical simulations with homogeneous and heterogeneous samples, and experimental results of drying cement specimens in the NMR [1], where drying was speeded up by the introduction of obstacles (aggregates) in cement paste. The choice of the size of LGA time-step is also important for the simulation of the drying process. In the homogeneous sample, the larger integration time is recommended and it should be at least 5000 [9], while for heterogeneous sample, the

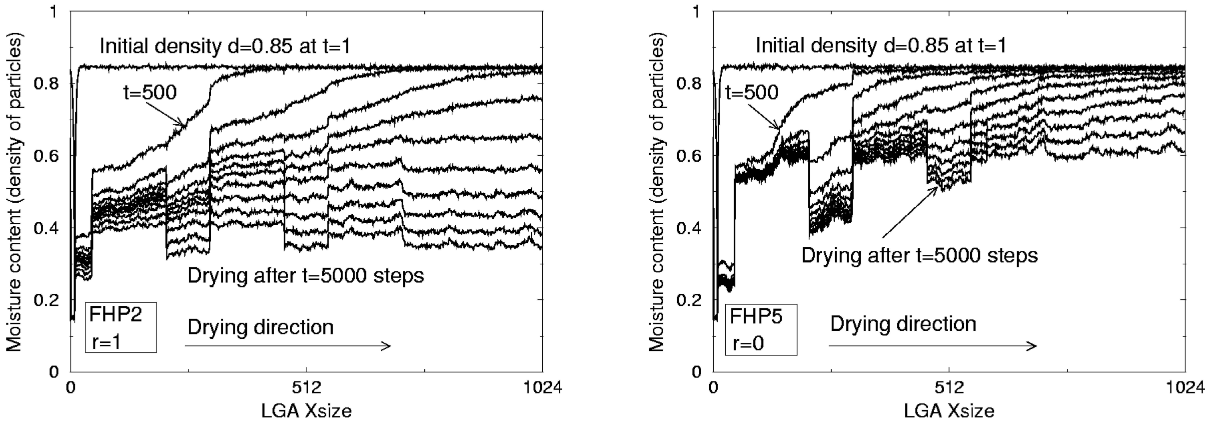

Figure 5. Moisture flow diagrams for model 2, with (left) FHP2 rule and specular-reflection (r = 1), and bounce-back reflection (r = 0) and FHP5 rule (right).

size can be much smaller, such as 500 steps. *Model 2 (addition of 6 larger obstacles).* The difference between model 1 and model 2 is the addition of six larger obstacles (160 x 160 lattice sites). They are located at fixed pre-determined positions (Fig. 4), closer to the drying surface, on the left side. Two boundary conditions are considered: bounce-back and specular-reflection as well as two collision rules: FHP2 (Figs 4, 5-left) and additional FHP5 (Fig. 5-right). Drying process can be speeded up by an increase in the number of collisions (quicker with FHP2 than with FHP5 due to the smaller viscosity of FHP2). Specular-reflection speeds up the drying (slip vs. no-slip boundary condition) regardless of the collision rule. In conclusion: the drying is the highest with specular-reflection and FHP2 rule (the collisions significantly reduce the first drying step) and the slowest with FHP5 rule and bounce-back reflection (Fig. 5-right). The important difference between samples with small and large obstacles is the jump in moisture content (Figs 3, 5), visible in the vicinity of every large obstacle. Around large obstacles, ITZ is created as a sort of a boundary layer, with a prescribed bounce-back collision rule among fluid and solid particles (obstacle). The 'jump' could be explained physically and mathematically. In drying, as a physical phenomenon, significant changes in the moisture gradient are expected in the boundary (bond zone between aggregate/matrix) as it is a highly porous medium and moisture flow occurs with higher velocity. The density of fluid particles and the velocity should have different values in the matrix (fluid particles) than in a zone between impermeable solids and fluid. The mathematical explanation comes from the Chapman-Enskog expansion and the Boltzmann equation. It is known that the Chapman-Enskog expansion is used to derive the macroscopic laws, when the Boltzmann equation is known. Although the Boltzmann equation is limited to dilute gases so it must be extended for higher collisions (BBGKY hierarchy), we can assume for the sake of argument that Boltzmann equation applies. In the continuous limit, the Boltzmann equation describes the behaviour of macroscopic quantities such as the density of fluid particles. It is an integro-differential equation of function f (r, v, t), which expresses how the number of molecules f (r, v, t) dr dv in the element (dr dv) of the six dimensional phase space, changes in time

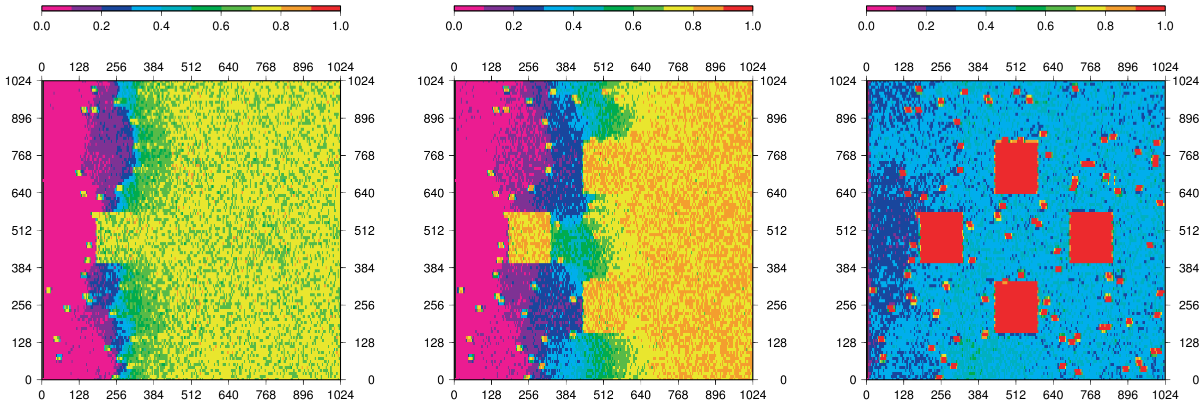

Figure 6. Model 3. LGA drying simulation in the heterogeneous sample, populated with 0.11% of solids, size (20 x 20) and four obstacles, symmetrically distributed, after (left) 500, (middle) 1000 and (right) 4000 LGA steps. FHP2 rule.

(t). This function gives the average number of particles in the differential area dr, having a velocity between v and dv. The quantity N_i [4] takes the role of the Boltzmann density function f, where the velocities are discrete in six directions (c_i) instead of a continuous variable v. The density of particle (ρ) is defined as an integral of f over the velocity v, such that density variations i.e. jumps (Figs 5, 7), present deviations in velocity. Hence, it should be expected to see a jump in density at the interfaces between solid obstacles and the surrounding fluid zone. The larger is the obstacle and subsequently ITZ area around it, the larger the jump. *Model 3 (addition of 4 larger obstacles).* The inclusion of four obstacles (Fig. 6) instead of six large obstacles, closer to the middle of the sample, contributes to rapid drying (Fig. 7), similarly as in homogeneous sample. Hence in drying simulation with heterogeneous LGA, it is not only the number of large obstacles and size of ITZ, but also their distance from the drying surface, that plays a role.

3. CONCLUDING REMARKS

Modeling of moisture flow (drying) by means of Lattice Gas Automata in 2-D is a successful numerical solution for Navier-Stokes in porous media, compared to Finite Element or Finite Difference Method and the complex experimental drying techniques. Several issues are influential in drying simulations with LGA heterogeneous models: number of the nodes in the lattice domain, the size (boundary) of the obstacles, and their placement to the drying surface, as well as boundary conditions and collision rules, and LGA drying time-step. The moisture gradient is influenced by the choice of the boundary conditions among fluid and solid particles (either bounce-back or specular-reflection), especially in the case where larger obstacles are present, as well as by the number of collisions i.e. specified collision rule. In model 1, with small randomly distributed solid particles, the moisture gradient (Fig. 3, left vs. right) does not depend significantly on the boundary rules, as it is the case with larger obstacles, which have larger boundary areas i.e. interface

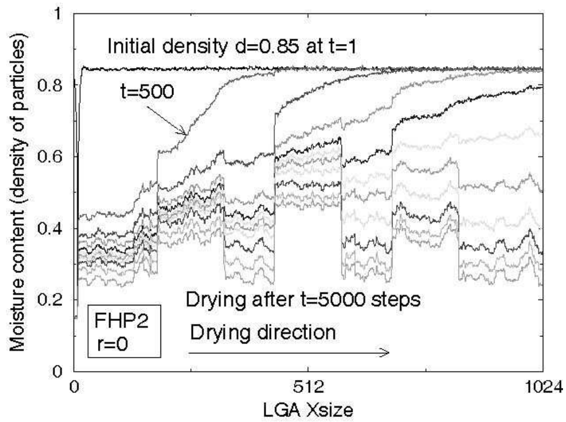

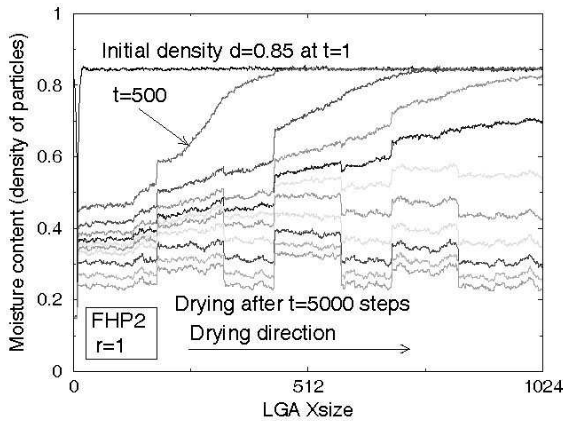

Figure 7. Moisture distribution in 5000 drying LGA time-steps with FHP2 rule, for model 3: (left) with bounce-back rule (r = 0) and (right) with specular reflection (r = 1).

zone (ITZ). The reason could be the ratio of the obstacle and ITZ size, to the size of the lattice. Area around obstacles can be again 'smooth' or 'rough', which can be simulated by the boundary conditions. From the experiments on drying, it is known that flow occurs through capillaries (up to 10 μm) and voids (10 nm and less). The roughness of the capillary walls may influence fluid flow, while the influence of void walls is negligible. If the capillary walls are smooth (simulation with a specular-reflection boundary), flow is expected to increase. On the contrary, flow is slower in rough capillaries, which is very similar to the simulation with bounce-back reflection. The speed of drying could be also controlled by the choice of collision rules. When the number of collisions is reduced by applying the FHP5 rule, instead of the FHP2 rule (compare Figs 5-left and 5-right), the speed of drying reduces. Speculations could be made regarding large moisture gradients in the vicinity of large aggregates, which could induce cracks on the sample surface. Crack could emerge by the positioning of larger number of aggregates closer to the surface, on a smaller distance from a surface. Cracks may also develop when aggregates are closely placed to each other, due to development of high moisture gradients on small distances. Although this appears to be confirmed in the literature [7], more experimental analyses are needed as well as extended coupling of a shrinkage and fracture model, with newly found drying shrinkage coefficient at low relative humidity values.

REFERENCES

1. Bisschop, J., Pel, L. and Van Mier, J.G.M., Mechanisms of Drying Shrinkage Microcracking in Concrete (the extended paper of contribution to ConCreep-6, Boston, USA), to appear in Cement and Concrete Research (2003)
2. Chopard, B. and Droz, M., Cellular Automata Modeling of Physical Systems, Cambridge University Press (1998)
3. d'Humieres, D. and Lallemand, P., Numerical Simulation of Hydrodynamics with Lattice Gas Automata in Two Dimensions, Complex Systems 1 599-632 (1987)

4. Frisch, U., Hasslacher, B. and Pomeau, Y., Lattice-Gas Automata for the Navier-Stokes Equation, Physical Review Letters, 56 (14) 1505-1508 (1986)
5. Frisch, U., d'Humieres, D., Hasslacher, B., Lallemand, P., Pomeau, Y. and Rivet, J-P., Lattice Gas Hydrodynamics in Two and Three Dimensions, Complex Systems 1 648-707 (1987)
6. Hsu, T.T.C., Slate, F.O., Sturman G.M. and Winter, G., Microcracking of Plain Concrete and the Shape of the Stress-Strain Curve, ACI Journal, Proc. 60 (2) 209-224 (1963)
7. Hsu, T.T.C., Mathematical Analysis of Shrinkage Stresses in a Model of Hardened Concrete, ACI Journal, Proc. 60 (3) 371-390 (1963)
8. Hsu, T.T.C. and Slate, F.O., Tensile Bond Strength between Aggregate and Cement Paste or Mortar, ACI Journal, Proc. 60 (4) 465-485 (1963)
9. Jankovic, D., Kuntz, M. and Van Mier, J.G.M., Numerical Analysis of Moisture Flow and Concrete Cracking by means of Lattice Type Models, in R. de Borst, J. Mazars, G. Pijaudier - Cabot and J.G.M. van Mier (eds.), Proc. 4th Intern. Conf. on Fracture Mechanics of Concrete and Concrete Structures 2001, Cachan, France, A.A. Balkema Publishers (1) 231-238 (2001)
10. Jankovic, D. and Van Mier, J.G.M., Crack Development in Concrete due to Moisture Flow, HERON 46 (3) 169-180 (2001)
11. Jankovic, D. and Van Mier, J.G.M., Preliminary Investigation of Drying Shrinkage Cement Paste Specimens, in R. Pyrz, J. Schjodt-Thomsen, J.C. Rauche, T. Thomsen and L.R. Jensen, Intern. Conf. on New Challenges in Mesomechanics 2002, Aalborg University, Denmark (1) 265-271 (2002)
12. Jankovic, D. and Van Mier, J.G.M., Drying of Porous Media: Numerical and Experimental Approach, in N. Bicanic, R. De Borst, H. Mang and G. Meschke (eds.), Computational Modeling of Concrete Structures, Proc. Euro-C Conference 2003, St. Johann im Pongau, Austria, A.A. Balkema Publishers 453-462 (2003)
13. Slate, F.O. and Olsefski, S., X-Rays for Study of Internal Structure and Microcracking of Concrete, ACI Journal, Proc. 60 (5) 575-588 (1963)
14. Wolf-Gladrow, D.A., Lattice-Gas Cellular Automata and Lattice Boltzmann Models, Springer (2000)
15. Wolfram, S., Cellular Automaton Fluids 1: Basic Theory, Journal of Statistical Physics 45 471-526 (1986)